Journal of the American Heart Association

ORIGINAL RESEARCH

Hemodynamic Change of Coronary Atherosclerotic Plaque After Statin Treatment: A Serial Follow-Up Study by Computed Tomography-Derived Fractional Flow Reserve

Mengmeng Yu, MD*; Xu Dai, MD*; Lihua Yu, MD; Zhigang Lu, MD; Chengxing Shen, MD; Xiaofeng Tao, MD; Jiayin Zhang, MD

BACKGROUND: Whether statin treatment can improve hemodynamic status of coronary atherosclerotic plaque remains unknown. It is of clinical interest to explore the hemodynamic change of coronary lesions after statin treatment.

METHODS AND RESULTS: Consecutive patients with intermediate pre-test probability of coronary artery disease were prospectively enrolled and underwent baseline coronary computed tomography angiography (CCTA) as well as follow-up CCTA. The primary end point was to determine the lesion-specific change of △computed tomography-derived fractional flow reserve (△CT-FFR, defined as the change of CT-FFR value across each lesion) after rosuvastatin treatment. The secondary end point was to compare the change of other plaque characteristics according to serial CCTA findings. 152 patients (mean age: 67.1±9.7 years, 100 men, mean follow-up duration of 13.9±2.5 months) were finally included. In non-calcified plaque subgroup, △CT-FFR was significantly lower at follow-up compared with baseline (0.051±0.010 versus 0.035±0.012, *P*=0.013). All other parameters were not found to be significantly different between baseline and follow-up CCTA measurements. In calcified plaque and mixed plaque subgroups, all parameters showed no significant differences between baseline and follow-up CCTA groups (*P*>0.05 for all). According to multivariate regression analysis, non-calcified plaque was >2 times more likely than calcified plaque to observe the decrease of △CT-FFR (adjusted hazard ratio: 2.05 [1.03–4.09], *P*=0.042).

CONCLUSIONS: In patients with mild to intermediate coronary stenosis, rosuvastatin treatment resulted in a reduction in lesion-specific △CT-FFR at mid-term follow-up. This hemodynamic improvement was mainly observed for non-calcified lesions.

Key Words: coronary artery disease ■ coronary CT angiography ■ fractional flow reserve ■ plaque ■ statin

Statin is commonly used for medical treatment in patients with coronary artery disease (CAD).[1] This lipid-lowering therapy is associated with reduction of high-risk plaque features and increase of plaque calcification, as observed by either intravascular ultrasound or coronary computed tomography angiography (CCTA).[2–5] However, whether this plaque components alteration after statin treatment will lead to the change of lesion-specific hemodynamic significance remains unknown.

Machine learning (ML)-based CT fractional flow reserve (CT-FFR) has been recently introduced as

Correspondence to: Jiayin Zhang, MD, Institute of Diagnostic and Interventional Radiology, Shanghai Jiao Tong University Affiliated Sixth People's Hospital, No. 600, Yishan Rd, Shanghai, China. E-mail: andrewssmu@msn.com

Supplementary Materials for this article are available at https://www.ahajournals.org/doi/suppl/10.1161/JAHA.120.015772

*Dr Mengmeng Yu and Dr Dai contributed equally to this work.

For Sources of Funding and Disclosures, see page 10.

JAHA is available at: www.ahajournals.org/journal/jaha

CLINICAL PERSPECTIVE

What Is New?

- Rosuvastatin treatment might potentially improve the hemodynamic status of coronary lesions with mild to moderate stenosis.
- Improvement in lesion-specific hemodynamic measures in response to rosuvastatin therapy seems to be most significant in non-calcified plaques.

What Are the Clinical Implications?

- Machine-learning based computed tomography-derived fractional flow reserve might be a useful approach to monitor the impact of statin treatment on different types of plaques.
- Non-calcified plaque is the phenotype that mostly benefits from statin treatment in regard to the improvement of hemodynamic significance.

Nonstandard Abbreviations and Acronyms

CAD	coronary artery disease
CCTA	coronary computed tomography angiography
DS	diameter stenosis
FFR	fractional flow reserve
LAP	low attenuation plaque
ML	machine learning
NRS	napkin-ring sign
PR	positive remodeling
TPV	total plaque volume

a time-saving and accurate approach for detecting ischemic coronary stenosis with reference to invasive FFR.[6–9] Considering that adverse plaque features are independently associated with decreased FFR value,[10,11] we hypothesized that the hemodynamic status of coronary stenosis would be improved after rosuvastatin treatment along with the reduction of high-risk plaque features. Therefore, the primary aim of the current study was to investigate the change of lesion-specific hemodynamic significance as determined by ML-based CT-FFR after rosuvastatin treatment.

MATERIALS AND METHODS

Patient Population

The data that support the findings of this study are available from the corresponding author upon reasonable request. Between April 2017 and December 2017, consecutive patients with chest pain were referred for CCTA to rule out obstructive disease. Patients were prospectively enrolled if they met the following inclusion criteria: (1) the pre-test probability of obstructive CAD was intermediate according to updated Diamond-Forrester score (defined as pre-test probability between 15% to 85%); (2) baseline CCTA revealed at least one lesion with stenotic extent from 30% to 70% on major epicardial arteries (diameter ≧2 mm); and (3) patients were referred for optimal medical treatment; and (4) patients agreed to undergo follow-up CCTA at 1-year to 1.5-year interval. The exclusion criteria were: (1) patients had previous history of myocardial infarction or coronary revascularization; (2) patients were contraindicated to the usage of iodine contrast media; (3) image quality of baseline or follow-up CCTA was severely impaired (in presence of severe artifact, non-diagnostic); (4) patients withdrew the informed consents during follow-up; (5) patients experienced major adverse cardiac events during follow-up; (6) patients refused to undergo follow-up CCTA; or (7) lost follow-up (Figure 1). The hospital ethics committee approved this prospective study and all patients gave written informed consent.

Sample Size Calculation

Because there was no published literature on the change of CT-FFR at 1-year follow-up after statin treatment. We determined the sample size based on our preliminary results of our own data. Before the enrollment of the current study, we have retrospectively reviewed 41 patients (55 lesions, not the current study) who underwent baseline and follow-up CCTA after rosuvastatin treatment. According to our preliminary results, the baseline △CT-FFR was 0.041±0.076 and the annual change of △CT-FFR was 0.0045±0.017 (10% greater than the baseline △CT-FFR). In light of the above findings, a total of 126 patients were required to achieve 90% power at a 1-sided 0.05 level of significance. When a drop-out rate of 10% was assumed, an enrollment of 139 subjects would be required. Ultimately, a total of 152 patients were enrolled, which provided >90% power to meet the primary end point.

Acquisition Protocol of CCTA

A third-generation dual source CT (SOMATOM Force, Siemens Healthineers, Germany) was used for CCTA imaging. Nitroglycerin was given sublingually in all patients before CCTA scan whereas beta-blocker was not used. Calcium score was firstly performed to calculate the calcification burden of each epicardial vessels. CCTA was performed by using a bolus tracking technique, with regions of interest placed in the descending aorta. A bolus of contrast media (40–55 mL) was injected into antecubital vein at the rate of 4 to 5 mL/s, followed by a

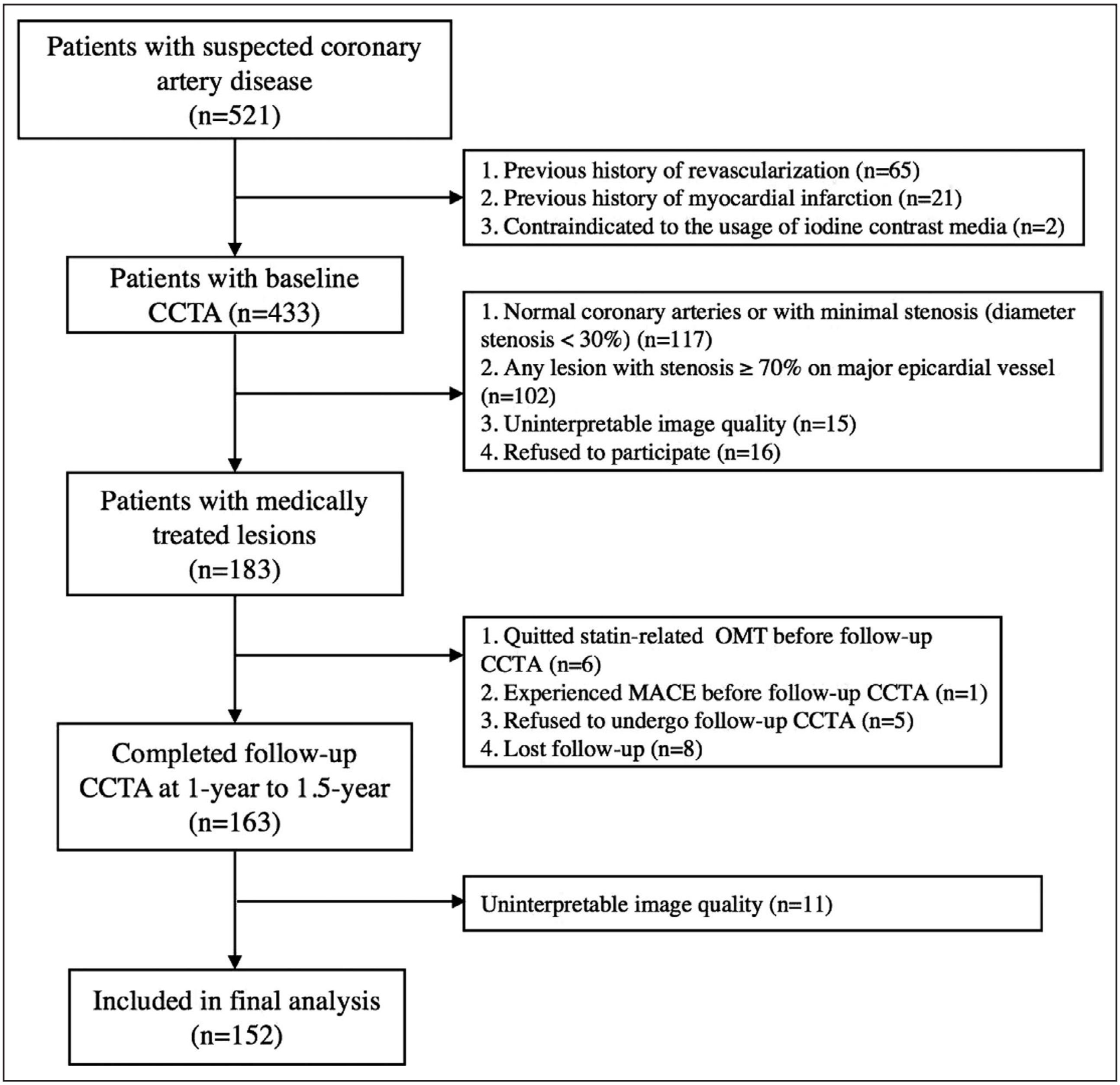

Figure 1. Flowchart of inclusion and exclusion.
CCTA indicates coronary computed tomography angiography; MACE, major adverse cardiac event; and OMT, optimal medical treatment.

40 mL saline flush by using dual-barrel power injector. Prospective ECG-triggered sequential acquisition was used in all patients with the triggering window covering from end-systolic to mid-diastolic phase (from 35% to 75% of R-R interval), with collimation=96×0.6 mm, reconstructed slice thickness=0.75 mm, reconstructed slice interval=0.5 mm, rotation time=250 ms and application of automated tube voltage and current modulation (CAREKv, CAREDose 4D, Siemens Healthineers, Germany). The reference tube current was set as 320 mAs and the reference tube voltage was set as 100 kVp. Same acquisition parameters were used for baseline and follow-up CCTA.

CT-Based Plaque Analysis

All CCTA data were reconstructed with a smooth kernel (Bv 40) and third generation iterative reconstruction technique (ADMIRE, strength level 3, Siemens Healthineers, Germany). The data set with best image quality was visually selected and transferred to an offline workstation (SyngoVia, Siemens Healthineers, Germany) for further evaluation.

Quantified plaque characterization was performed semi-automatically by using a dedicated plaque analysis software (Coronary Plaque Analysis, version 2.0, Siemens Healthineers). As previously reported, the presence of atherosclerosis was defined as any tissue ≥1 mm^2 within or adjacent to the lumen that could be discriminated from surrounding pericardial, epicardial fat, or lumen, and identified in >2 planes.[12] Various parameters were measured as follow: (1) minimal lumen diameter; (2) diameter stenosis (DS); (3) lesion length; (4) remodeling index, positive remodeling (PR) was defined as a remodeling index ≥1.1[13]; (5) low-attenuation plaque (LAP) as defined by previous study[13]; (6) spotty calcification; (7) Napkin-ring sign (NRS) as defined by previous study[14]; (8) total plaque volume (TPV). Detailed definitions of the above parameters were given in Data S1. In addition, all target lesions were visually assigned to 1 of 3 categories as previously described: non-calcified, calcified or mixed (both non-calcified and calcified components present).[15]

Two cardiovascular radiologists (with 12- and 4-year experience of cardiac imaging) independently analyzed the above parameters and the mean values of measurement were used for further analysis. The intra-observer and inter-observer agreement of all parameters was assessed by intraclass correlation coefficients in 40 randomly selected cases.

CT-FFR Analysis

The present study used an ML-based algorithm for CT-FFR simulation (cFFR, version 3.0, Siemens Healthineers, Forchheim, Germany), which was research software and not commercially available. This model was trained on a large database of synthesized coronary anatomies, where the reference values are computed using a computational fluid dynamics based model.[16] Previous clinical studies have validated the diagnostic performance of this method with reference to invasive FFR.[6,7] The details about how this ML-based model was trained and how onsite processing was performed were given in Data S1.

The lesion-specific CT-FFR values were measured at the distal shoulder of the lesion, where no plaque could be detected. In addition, the change in CT-FFR value across the lesion (△CT-FFR) was also calculated for each lesion by computing the difference between the proximal and distal CT-FFR values as follows: $\triangle\text{CT-FFR}=\text{CT-FFR}_{\text{proximal}}-\text{CT-FFR}_{\text{distal}}$. As previously reported in EMERALD study, △CT-FFR was introduced to more accurately evaluate the lesion-specific hemodynamic significance in the presence of tandem lesions and this parameter had prognostic value for predicting culprit lesions.[17] The CT-FFR and △CT-FFR values of all targeting lesions were calculated independently by two cardiovascular radiologists (with 12- and 4-year experience of cardiac imaging). The mean values were used for analysis.

Clinical Follow-Up and Study End Points

All recruited patients were referred for rosuvastatin treatment (Crestor, AstraZeneca China, 10 or 20 mg daily) according to the 2013 American guideline on the treatment of blood cholesterol to reduce atherosclerotic cardiovascular risk in adults.[18] The details of rosuvastatin treatment were given in Data S1. Follow-up CCTA was performed in all patients at 1- to 1.5-year interval. The primary objective of the current study was to determine the lesion-specific change of baseline △CT-FFR and follow-up △CT-FFR values after rosuvastatin treatment. The secondary objective was to compare the change of other plaque characteristics according to baseline and follow-up CCTA findings.

Statistical Analysis

Statistical analysis was performed using commercially available statistical analysis software (MedCalc Statistical Software version 15.2.2, MedCalc Software bvba, Ostend, Belgium and R version 3.3.0 software, Vienna, Austria). One-sample Kolmogorov–Smirnov test was used to check the assumption of normal distribution. Quantitative variables with normal distribution were expressed as means±SD while median and quartiles were used otherwise. Categorical variables were reported as count (%) and compared by the Fisher exact test or Chi-square test, according to the data cell size. Student *t*-test was used for normally distributed data, and the Mann–Whitney *U* test was used for data that were not normally distributed. Inter-observer and intra-observer variability of CCTA-derived plaque features was assessed by intraclass correlation coefficient. Bland-Altman analysis was performed to test the difference between observer 1 and observer 2. The effect of the variables on the decrease of △CT-FFR at follow-up CCTA was evaluated using the univariable and multivariable Cox regression models. In multivariable Cox regression analyses, 2 models were used to adjust with the increasing degrees of potential confounding factors at baseline. Model 1 was adjusted for traditional risk factors, including age, sex, diabetes mellitus, dyslipidemia, hypertension, current smoker, and family history of CAD. Model 2 was further adjusted for low attenuation plaque, spotty calcification, remodeling index, napkin-ring sign, diameter stenosis, Agatston calcium score, total plaque volume, calcified plaque volume, non-calcified plaque volume, and △CT-FFR at baseline. Statistical significance was defined as a 2-sided $P<0.05$.

RESULTS

Clinical Characteristics

From April 2017 to December 2017, 521 patients with suspected coronary artery disease were initially screened. Of those patients, 369 patients, who did not meet the inclusion criteria, were excluded from the enrollment. The detailed reasons for exclusion were listed in Figure 1. Finally, a total of 152 patients completed 1- to

1.5-year follow-up CCTA and were included for further analysis (mean age: 67.1±9.7 [range 39–91] years), 100 men mean age: 69.5±10.9 (range 39–90) years, and 52 women (mean age: 65.1±8.3 [range 43–91] years). Detailed demographic data are given in Table 1.

Follow-up CCTA was performed with a mean interval of 13.9±2.5 months. The mean processing time for CT-FFR calculation was 9.1±3.2 minutes. The radiation dose and contrast media used for baseline and follow-up CCTA was shown in Table 2.

Comparison of Coronary Plaque Features Between Baseline and Follow-Up CCTA

The inter-observer and intra-observer agreement for baseline and follow-up CCTA-derived plaque features were concordant (Tables S1 and S2). The Bland–Altman analysis showed good agreement between observer 1 and observer 2 for △CT-FFR measurement with a mean difference of 0.001 (95% CI, 0.023 to −0.020) (Figure S1). Focal Agatston score, minimal lumen diameter, diameter stenosis, total lesion length, TPV, calcified plaque volume, non-calcified plaque volume, LAP, LAP volume, spotty calcification, positive remodeling, napkin-ring sign as well as △CT-FFR were not found to be significantly different between baseline and follow-up CCTA findings (*P*>0.05 for all, Table 3).

Subgroup Analysis of CCTA-Derived Parameters on Coronary Plaque Types

Comparison of coronary plaque characteristics between baseline and follow-up CCTA according to different plaque types are summarized in Table 4. In non-calcified plaque subgroup, △CT-FFR was significantly lower at follow-up compared with baseline (0.051±0.010 versus 0.035±0.012, *P*=0.013, Figures 2 and 3). Other parameters, such as minimal lumen diameter, diameter stenosis, total lesion length, TPV, calcified plaque volume, non-calcified plaque volume, LAP, LAP volume, spotty

Table 1. Baseline Characteristics

Age, y	67.1±9.7
Men	100 (65.8%)
Body mass index, kg/m^2	21.1±2.0
Risk factors	
Hypertension	68 (44.7%)
Diabetes mellitus	54 (35.5%)
Dyslipidemia	57 (37.5%)
Current smoker	27 (17.7%)
Family history of CAD	12 (7.9%)
Medication in use	
Statin	152 (100.0%)
Aspirin	91 (59.8%)
Nitrate	132 (86.8%)
ACE inhibitor/ARB	81 (53.2%)
Clopidogrel	61 (40.13%)
Beta-blocker	102 (67.1%)
Calcium antagonist	91 (59.9%)

Values are mean±SD, n (%), or median (interquartile range). ACE indicates angiotensin-converting enzyme; ARB, angiotensin receptor blocker; and CAD, coronary artery disease.

Table 2. Clinical Characteristics

	Baseline (n=152)	Follow-Up (n=152)	*P* Value*
Angina[†]			
CCS I	100 (65.8%)	107 (70.4%)	0.39
CCS II	52 (34.2%)	45 (29.6%)	0.39
Biochemical assessment			
TC, mmol/L	4.56 [3.89–7.13]	4.28 [3.45–4.98]	0.023
HDL-C, mmol/L	1.29 [1.06–1.54]	1.29 [1.06–1.62]	0.88
LDL-C, mmol/L	3.52 [2.92–4.67]	3.89 [3.10–4.12]	0.45
Triglycerides, mmol/L	1.46 [0.89–5.00]	1.06 [0.81–2.55]	0.21
HbA1c, %	5.9 [5.10–6.60]	5.7 [5.10–6.20]	0.39
CRP, mg/L	2.57 [0.65–5.52]	2.14 [1.10–5.11]	0.92
Contrast media used for CCTA, mL	50.6±11.3	51.2±12.4	0.96
Radiation dose of CCTA, mSv	3.8 [2.7–5.9]	4.19 [2.81–6.14]	0.81

CCS indicates Canadian Cardiovascular Society; CCTA, coronary computed tomography angiography; CRP, C-reactive protein; HDL-C, high-density lipoprotein cholesterol; LDL-C, low-density lipoprotein cholesterol; and TC, total cholesterol.

*Baseline vs follow-up.

†Angina was assessed according to the Canadian Cardiovascular Society Functional Classification of Angina Pectoris.

Table 3. Comparison of Coronary Plaque Features Between Baseline and Follow-Up CCTA

	Baseline (n=194)	Follow-Up (n=194)	*P* Value*
Focal Agatston score	60.20 [0–175]	61.00 [0–170]	0.99
MLD, mm	1.97±0.51	1.98±0.51	1.00
Diameter stenosis, %	49.30±14.80	48.00±16.80	0.45
Total lesion length, mm	10.74 [6.70–19.20]	10.2 [6.80–19.30]	0.67
TPV, mm^3	112.50 [50.40–254.60]	108.30 [50.40–249.40]	1.00
Calcified PV, mm^3	23.90 [0–98.40]	25.70 [0–99.50]	0.87
No-calcified PV, mm^3	51.30 [0–148.00]	49.90 [0–149.20]	0.87
LAP	36 (18.60%)	31 (16.00%)	0.51
LAP volume, mm^3	0 [0–0]	0 [0–0]	0.55
Napkin-ring sign	55 (28.40%)	54 (27.80%)	0.91
Spotty calcification	18 (9.30%)	19 (9.80%)	1.00
Remodeling index	1.13±0.20	1.12±0.21	0.82
ΔCT-FFR	0.054±0.015	0.049±0.016	0.11

CCTA indicates coronary computed tomography angiography; CT, computed tomography; FFR, fractional flow reserve; LAP, low attenuation plaque; MLD, minimal lumen diameter; PV, plaque volume; and TPV, total plaque volume.

*Baseline vs follow-up.

Table 4. Comparison of Coronary Plaque Features Between Baseline and Follow-Up CCTA: Subgroup Analysis With Regard to Different Types of Plaque

	Baseline	Follow-Up	*P* Value
Non-calcified plaque (n=73)			
Focal Agatston score	···	···	···
MLD, mm	2.00±0.47	1.99±0.48	0.83
Diameter stenosis, %	47.00±15.00	43.00±18.00	0.18
Total lesion length, mm	8.50 [6.50–12.50]	8.10 [6.30–12.30]	0.51
TPV, mm^3	84.30 [45.50–181.00]	82.20 [44.50–173.00]	0.99
Calcified PV, mm^3	···	···	···
No-calcified PV, mm^3	84.30 [45.50–181.00]	82.20 [44.50–173.00]	0.99
LAP	30 (41.00%)	24 (32.90%)	0.25
LAP volume, mm^3	0 [0–8.10]	0 [0–5.40]	0.64
Napkin-ring sign	30 (41.10%)	31 (42.50%)	0.76
Spotty calcification	4 (5.50%)	5 (6.80%)	1.00
Remodeling index	1.08±0.17	1.09±0.17	0.85
ΔCT-FFR	0.051±0.010	0.035±0.012	0.013
Calcified plaque (n=54)			
Focal Agatston score	230.50 [135.00–382.00]	232.50 [137.00–382.00]	1.00
MLD, mm	1.99±0.56	2.00±0.55	0.97
Diameter stenosis, %	48.40±14.00	48.00±15.00	0.97
Total lesion length, mm	19.10 [8.20–27.10]	17.80 [8.50–27.40]	0.92
TPV, mm^3	100.45 [59.10–254.60]	99.54 [58.10–255.10]	0.88
Calcified PV, mm^3	100.45 [59.10–254.60]	99.54 [58.1–255.10]	0.88
No-calcified PV, mm^3	···	···	···
LAP	···	···	···
LAP volume, mm^3	···	···	···
Napkin-ring sign	···	···	···
Spotty calcification	···	···	···
Remodeling index	1.20±0.20	1.19±0.21	0.96
ΔCT-FFR	0.048±0.011	0.045±0.012	0.84
Mixed plaque (n=67)			
Focal Agatston score	96.00 [52.40–173.50]	97.00 [52.50–177.20]	0.95
MLD, mm	1.91±0.52	1.89±0.52	0.57
Diameter stenosis, %	58.00 [41.00–67.00]	54.00 [40.00–68.00]	0.92
Total lesion length, mm	11.90 [7.14–19.00]	11.20 [6.95–17.80]	0.92
TPV, mm^3	181.60 [51.90–353.10]	178.60 [48.90–363.30]	0.99
Calcified PV, mm^3	53.50 [20.00–115.40]	54.60 [20.20–115.90]	0.88
No-calcified PV, mm^3	102.00 [31.00–197.60]	101.30 [29.00–209.50]	0.95
LAP	6 (9.00%)	7 (10.40%)	0.77
LAP volume, mm^3	0 [0–0]	0 [0–0]	0.79
Napkin-ring sign	25 (37.30%)	23 (34.30%)	0.71
Spotty calcification	14 (20.90%)	12 (17.90%)	0.66
Remodeling index	1.11±0.21	1.11±0.20	0.98
ΔCT-FFR	0.063±0.014	0.064±0.016	0.67

CCTA indicates coronary computed tomography angiography; CT, computed tomography; FFR, fractional flow reserve; LAP, Low attenuation plaque; MLD, minimal lumen diameter; PV, plaque volume; and TPV, total plaque volume.

calcification, positive remodeling, napkin-ring sign, were not found to be significantly different between baseline and follow-up CCTA measurements (Table 4). In calcified plaque and mixed plaque subgroups, all parameters showed no significant differences between baseline and follow-up CCTA groups (P>0.05 for all) (Table 4, Figure 4).

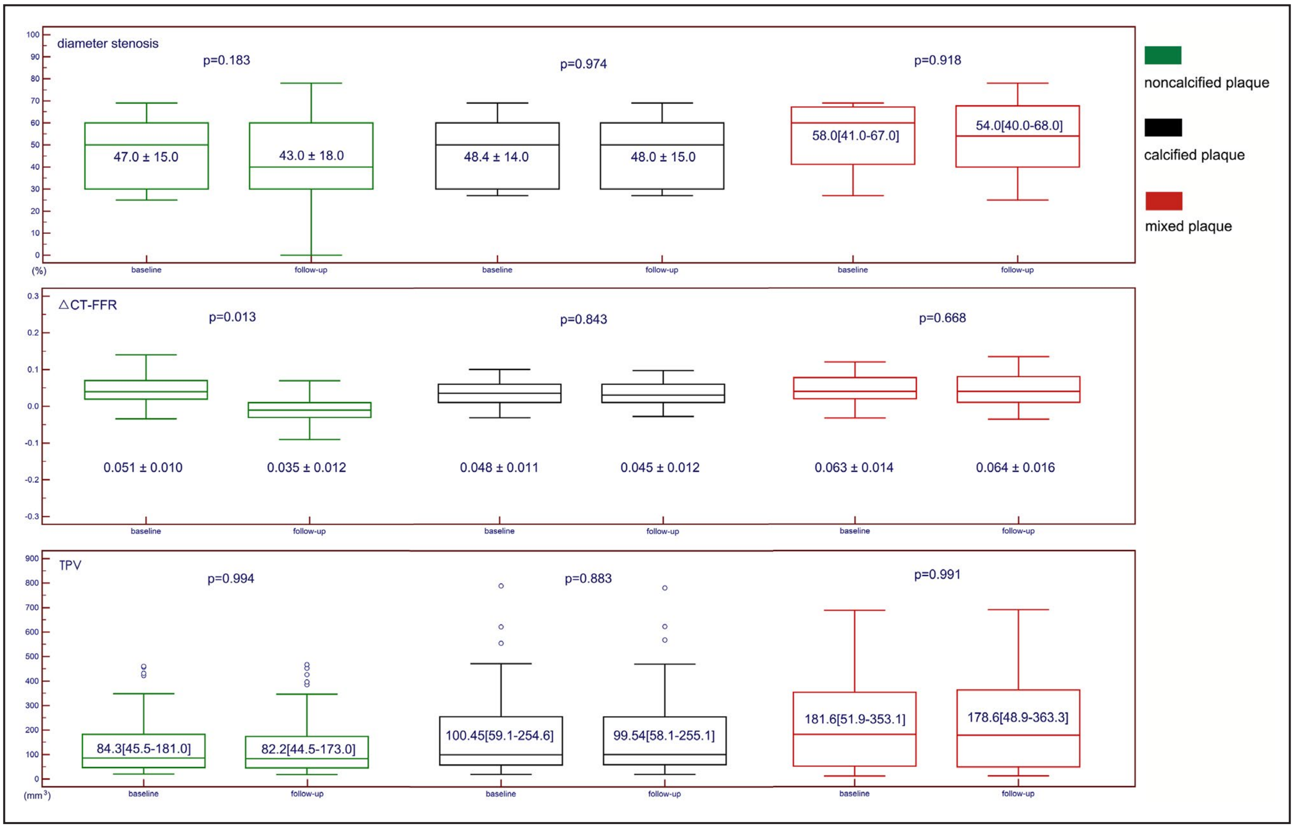

Figure 2. Box plot showing the dynamic change of diameter stenosis, △CT-FFR and total plaque volume after statin treatment in different subgroups.
CT indicates computed tomography; FFR, fractional flow reserve; and TPV, total plaque volume.

Univariable and Multivariable Cox Regression Analyses

Univariable and multivariable Cox regression analyses were performed to determine whether the association between the decrease of △CT-FFR and coronary plaque types is independent of cardiovascular risk factors and CAD characteristics. In univariable analysis, non-calcified plaque was significantly associated with lower △CT-FFR at follow-up CCTA. Compared with calcified plaque, non-calcified plaque was >2 times more likely to observe lower △CT-FFR (unadjusted hazard ratio: 2.02 [1.12–3.65], P=0.02) after rosuvastatin treatment. In multivariable regression analysis, the association between non-calcified plaque and lower △CT-FFR was consistently observed after adjusting for traditional cardiovascular risk factors and CAD characteristics. Univariable and multivariable Cox regression analyses are summarized in Tables 5 and 6.

DISCUSSION

The major finding of the current study demonstrated that rosuvastatin treatment might potentially improve the hemodynamic status of coronary lesions with mild to moderate stenosis. This improvement was observed exclusively in the subgroup of non-calcified plaques, regardless of the change of LAP volume and TPV.

Statin treatment is able to stabilize vulnerable coronary atherosclerotic plaques and slow lesion progression according to previous landmark studies by serial intravascular ultrasound imaging.[19,20] This protective effect has also been confirmed by 1 large-scale multi-center CCTA study, showing the decrease of non-calcified component and increase of plaque calcification.[4] However, no prior studies have investigated the hemodynamic change of statin-treated plaques via serial follow-up imaging modalities. To complement the above findings, the current study made one step further to focus on the improvement of hemodynamic status because of rosuvastatin treatment. In contrast to the insignificant reduction of LAP volume and TPV, lower △CT-FFR values were noted in non-calcified plaques, indicating the improvement of lesion-specific hemodynamic status. This reversion effect of hemodynamic significance was also observed irrelevantly to the change of DS and could be potentially ascribed to the synergetic effect of the following factors. First, high-risk plaque features, such as presence of LAP and PR, were reported to be associated with reduced FFR regardless of the degree of DS.[10,11] At the site of a lesion with large necrotic core and extraluminal

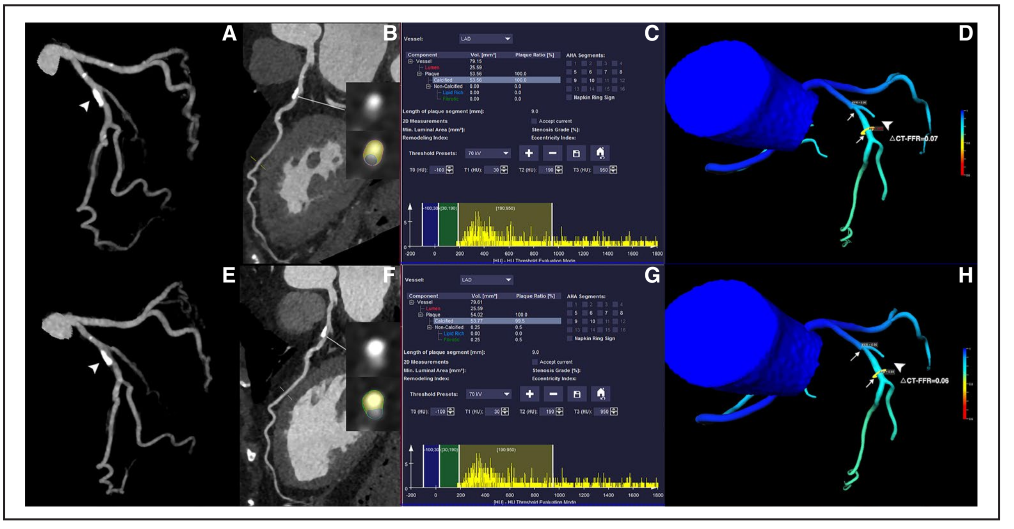

Figure 3. Representative case of a 53-year old man showing decreased △computed tomography-fractional flow reserve after statin treatment.
A through **D**, The baseline CCTA revealed moderate stenosis of proximal RCA (white arrowhead). The TPV was 61.9 mm^3 and △computed tomography-fractional flow reserve of this lesion was 0.07. **E** through **H**, The follow-up CCTA (13 months later) after statin treatment showed mild stenosis of proximal RCA (white arrowhead). The plaque regression was also observed and TPV was 18.66 mm^3. Follow-up △computed tomography-fractional flow reserve was significantly reduced to 0.01 after statin treatment. CCTA indicates coronary computed tomography angiography; CT, computed tomography; FFR, fractional flow reserve; RCA, right coronary artery; and TPV, total plaque volume.

expansion, impaired vasodilatory capacity may prevent the stenotic vascular segment to dilate to the same extent as the rest of the vessel and consequently result in a relative pressure drop at the time of maximal hyperemia.[21] In the present study, rosuvastatin treatment tended to insignificantly reduce LAP volume, which

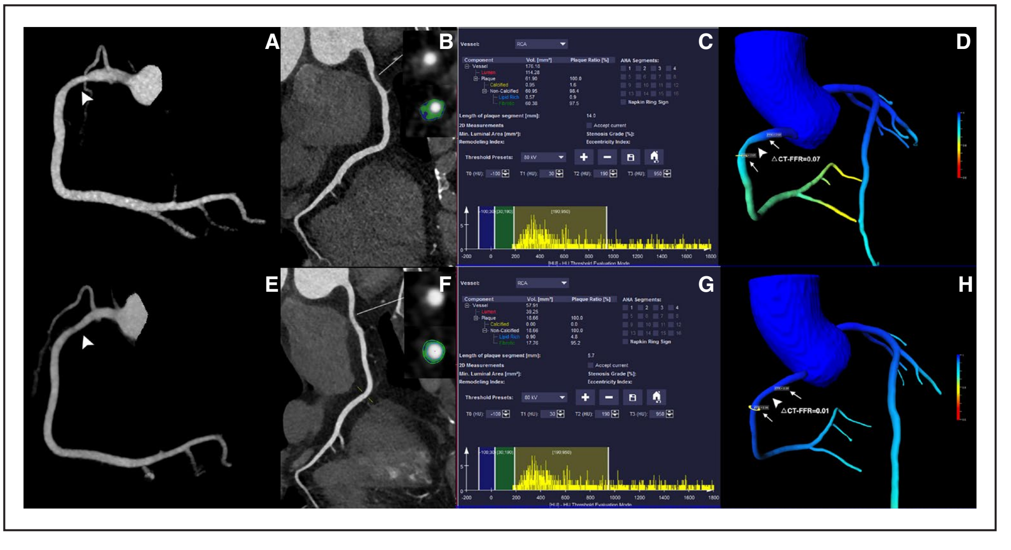

Figure 4. Representative case of a 77-year-old woman showing similar △computed tomography-fractional flow reserve after statin treatment.
A through **D**, The baseline coronary computed tomography angiography revealed calcified lesion with mild stenosis of proximal left anterior descending (white arrowhead). The total plaque volume was 53.56 mm^3 and △computed tomography-fractional flow reserve of this lesion was 0.07. **E** through **H**, The follow-up coronary computed tomography angiography (14 months later) after statin treatment showed mild stenosis of proximal left anterior descending (white arrowhead). The total plaque volume was 53.77 mm^3 and follow-up △computed tomography-fractional flow reserve was 0.06, which were both similar to baseline measurements. CCTA indicates coronary computed tomography angiography; CT, computed tomography; FFR, fractional flow reserve; LAD, left anterior descending; and TPV, total plaque volume.

Table 5. Univariable Cox Regression Analyses: the Effects of Traditional Risk Factors and CAD Characteristics on the Decrease of △CT-FFR at Follow-Up CCTA

	Univariate	
	Unadjusted HR [95% CI]	*P* Value
Age (per+1 y)	1.00 [0.98–1.02]	0.94
Men	0.94 [0.61–1.46]	0.79
Diabetes mellitus	0.71 [0.43–1.17]	0.18
Dyslipidemia	0.89 [0.54–1.47]	0.65
Hypertension	1.09 [0.71–1.68]	0.70
Current smoker	1.56 [0.94–2.61]	0.09
Family history of CAD	1.01 [0.72–1.88]	0.81
LAP(+) at baseline	1.49 [0.91–2.44]	0.12
SC(+) at baseline	0.76 [0.33–1.75]	0.52
RI at baseline	0.73 [0.25–2.15]	0.57
NRS(+) at baseline	1.17 [0.76–1.82]	0.49
DS at baseline	2.47 [0.56–10.93]	0.23
Agatston calcium score at baseline	1.00 [0.99–1.01]	0.92
TPV at baseline	1.00 [0.99–1.01]	0.98
Calcified PV at baseline	1.00 [0.99–1.01]	0.81
Non-calcified PV at baseline	1.00 [0.99–1.01]	0.78
△CT-FFR at baseline	16.33 [0.64–41.35]	0.09
Plaque type		
Calcified	Reference	···
Noncalcified	2.02 [1.12–3.65]	0.021
Mixed	1.45 [0.77–2.73]	0.25

CAD indicates coronary artery disease; CCTA, coronary computed tomography angiography; CT, computed tomography; DS, diameter stenosis; FFR, fractional flow reserve; HR, hazard ratio; LAP, low attenuation plaque; NRS, napkin-ring sign; PV, plaque volume; RI, remodeling index; SC, spotty calcification; and TPV, total plaque volume.

Table 6. Multivariable Cox Regression Analyses: the Effects of Traditional Risk Factors and CAD Characteristics on the Decrease of △CT-FFR at Follow-Up CCTA

	Multivariate*		Multivariate†	
	Adjusted HR [95% CI]	*P* Value	Adjusted HR [95% CI]	*P* Value
Plaque type				
Calcified PV	Reference	···	Reference	···
Non-calcified PV	2.12 [1.08–4.17]	0.030	2.05 [1.03–4.09]	0.042
LAP volume	1.46 [0.74–2.85]	0.27	1.44 [0.74–2.79]	0.28

CAD indicates coronary artery disease; CCTA, coronary computed tomography angiography; CT, computed tomography; FFR, fractional flow reserve; HR, hazard ratio; LAP, low attenuation plaque; and PV, plaque volume.

*Model 1: adjustment for age, sex, diabetes mellitus, dyslipidemia, hypertension, current smoker, family history of CAD.

†Model 2: further adjustment for low attenuation plaque, spotty calcification, remodeling index, napkin-ring sign, diameter stenosis, Agatston calcium score, total plaque volume, calcified plaque volume, non-calcified plaque volume, △CT-FFR at baseline.

is theoretically associated with impaired vasodilatory capacity and lower CT-FFR values. Second, mildly smaller TPV and shorter lesion length were also noted on follow-up CCTA. According to the Poiseuille equation, resistance to flow through a narrowed vessel is directly to the length of the narrowing.[22] Thus, this geometric change will also lead to higher CT-FFR values. With the synergetic effect of the above 2 mechanisms, it is reasonable to expect hemodynamic improvement of coronary stenosis post rosuvastatin treatment.

According to the subgroup analysis, it is also of note that hemodynamic improvement was not observed in the subgroup of calcified plaques and mixed plaques. In other words, rosuvastatin treatment did not reduce lesion-specific △CT-FFR values in those subgroups, which could be found for non-calcified lesions. This finding complements the results of previous studies that statin is more effective for non-calcified plaques.[15,23] In contrast, for calcium burdens, statin therapy demonstrated no impact on slowing the progression of coronary artery calcium score.[24,25]

In light of the above findings, the clinical implication of the current study lies in using ML-based CT-FFR for serial follow-up of medically treated coronary lesions. As nicely shown by current results, CCTA combined with ML-based CT-FFR was able to not only evaluate the change of plaque composition but also quantify the hemodynamic improvement after rosuvastatin treatment. In contrast to the invasive nature of intravascular ultrasound and optical coherence tomography, CCTA is more acceptable in low to intermediate-risk patients and easier to be accessed than those invasive imaging modalities. In addition, the present study also revealed that non-calcified plaque benefits the most from rosuvastatin treatment than does calcified and mixed plaque. This finding could potentially support the use of CCTA for guiding more individualized medical treatment according to its plaque characterization.

Despite the above promising findings, the current study has several limitations. First, the primary end point of this study was the change of lesion specific CT-FFR after rosuvastatin treatment rather than other hard events, such as all-cause mortality and myocardial infarction. Besides, the current cohort was not followed up after the second CCTA so that it was not possible to determine the correlation of △CT-FFR and major adverse cardiac events. Therefore, future prospective studies with larger sample size and longer follow-up period are warranted to investigate the relationship between CT-FFR improvement and prognosis. Second, the change of lesion-specific hemodynamic significance was evaluated by ML-based CT-FFR instead of invasive FFR. Although this CT-FFR simulation algorithm is considered perform well with reference to invasive FFR,[6,7] however, the diagnostic performance of ML-based CT-FFR could be impaired for "grey-zone" lesions (lesions with CT-FFR values between 0.7 to 0.8).[8] Nevertheless, invasive FFR is much less accessible in a large-scale follow-up study. Therefore, CT-FFR is still the most reasonable tool to monitor medical treatment effect. Finally, the statin dosage was not unified (all patients were treated with rosuvastatin but at different dosages), which could lead to varied extent of progression/regression across population. This issue needs to be further addressed in future prospective study with high-intensity statin treatment only.

CONCLUSIONS

Rosuvastatin treatment was able to reduce lesion-specific ΔCT-FFR at mid-term follow-up. This hemodynamic improvement was mainly observed for non-calcified lesions.

ARTICLE INFORMATION

Received January 1, 2020; accepted April 2, 2020.

Affiliations

From the Institute of Diagnostic and Interventional Radiology (M.Y., X.D., L.Y., J.Z.) and Department of Cardiology (Z.L., C.S.), Shanghai Jiao Tong University Affiliated Sixth People's Hospital, Shanghai, China; Department of Radiology, Shanghai Ninth People's Hospital, Shanghai Jiao Tong University School of Medicine, Shanghai, China (X.T.).

Sources of Funding

This study is supported by National Natural Science Foundation of China (grant no.: 81671678), Medical Guidance Scientific Research Support Project of Shanghai Science and Technology Commission (grant no.: 19411965100), Shanghai Key Discipline of Medical Imaging (no.: 2017ZZ02005) and Innovative Research Team of High-Level Local Universities in Shanghai.

Disclosures

None.

Supplementary Materials

Data S1
Tables S1–S2
Figure S1

REFERENCES

1. Ridker PM, Danielson E, Fonseca FA, Genest J, Gotto AM Jr, Kastelein JJ, Koenig W, Libby P, Lorenzatti AJ, MacFadyen JG, et al. Rosuvastatin to prevent vascular events in men and women with elevated C-reactive protein. *N Engl J Med*. 2008;359:2195–2207.
2. Kini AS, Baber U, Kovacic JC, Limaye A, Ali ZA, Sweeny J, Maehara A, Mehran R, Dangas G, Mintz GS, et al. Changes in plaque lipid content after short-term intensive versus standard statin therapy: the YELLOW trial (reduction in yellow plaque by aggressive lipid-lowering therapy). *J Am Coll Cardiol*. 2013;62:21–29.
3. Takayama T, Komatsu S, Ueda Y, Fukushima S, Hiro T, Hirayama A, Saito S; ALTAIR study group. Comparison of the effect of rosuvastatin 2.5 mg vs 20 mg on coronary plaque determined by angioscopy and intravascular ultrasound in Japanese with stable angina pectoris (from the Aggressive Lipid-Lowering Treatment Approach Using Intensive Rosuvastatin for Vulnerable Coronary Artery Plaque [ALTAIR] Randomized Trial). *Am J Cardiol*. 2016;117:1206–1212.
4. Lee SE, Chang HJ, Sung JM, Park HB, Heo R, Rizvi A, Lin FY, Kumar A, Hadamitzky M, Kim YJ, et al. Effects of statins on coronary atherosclerotic plaques: the PARADIGM study. *JACC Cardiovasc Imaging*. 2018;11:1475–1484.
5. Auscher S, Heinsen L, Nieman K, Vinther KH, Løgstrup B, Møller JE, Broersen A, Kitslaar P, Lambrechtsen J, Egstrup K. Effects of intensive lipid-lowering therapy on coronary plaques composition in patients with acute myocardial infarction: assessment with serial coronary CT angiography. *Atherosclerosis*. 2015;24:579–587.
6. Tesche C, De Cecco CN, Baumann S, Renker M, McLaurin TW, Duguay TM, Bayer RR II, Steinberg DH, Grant KL, Canstein C, et al. Coronary CT angiography-derived fractional flow reserve: machine learning algorithm versus computational fluid dynamics modeling. *Radiology*. 2018;288:64–72.
7. Coenen A, Kim YH, Kruk M, Tesche C, De Geer J, Kurata A, Lubbers ML, Daemen J, Itu L, Rapaka S, et al. Diagnostic accuracy of a machine-learning approach to coronary computed tomographic angiography-based fractional flow reserve: result from the MACHINE Consortium. *Circ Cardiovasc Imaging*. 2018;11:e007217.
8. Yu M, Lu Z, Li W, Wei M, Yan J, Zhang J. CT morphological index provides incremental value to machine learning based CT-FFR for predicting hemodynamically significant coronary stenosis. *Int J Cardiol*. 2018;265:256–261.
9. Yu M, Lu Z, Shen C, Yan J, Wang Y, Lu B, Zhang J. The best predictor of ischemic coronary stenosis: subtended myocardial volume, machine learning-based FFR_{CT}, or high-risk plaque features? *Eur Radiol*. 2019;29:3647–3657.
10. Park HB, Heo R, Ó Hartaigh B, Cho I, Gransar H, Nakazato R, Leipsic J, Mancini GBJ, Koo BK, Otake H, et al. Atherosclerotic plaque characteristics by CT angiography identify coronary lesions that cause ischemia: a direct comparison to fractional flow reserve. *JACC Cardiovasc Imaging*. 2015;8:1–10.
11. Gaur S, Øvrehus KA, Dey D, Leipsic J, Bøtker HE, Jensen JM, Narula J, Ahmadi A, Achenbach S, Ko BS, et al. Coronary plaque quantification and fractional flow reserve by coronary computed tomography angiography identify ischaemia-causing lesions. *Eur Heart J*. 2016;37:1220–1227.
12. Budoff MJ, Dowe D, Jollis JG, Gitter M, Sutherland J, Halamert E, Scherer M, Bellinger R, Martin A, Benton R, et al. Diagnostic performance of 64-multidetector row coronary computed tomographic angiography for evaluation of coronary artery stenosis in individuals without known coronary artery disease: results from the prospective multicenter ACCURACY (Assessment by Coronary Computed Tomographic Angiography of Individuals Undergoing Invasive Coronary Angiography) trial. *J Am Coll Cardiol*. 2008;52:1724–1732.
13. Motoyama S, Sarai M, Harigaya H, Anno H, Inoue K, Hara T, Naruse H, Ishii J, Hishida H, Wong ND, et al. Computed tomographic angiography characteristics of atherosclerotic plaques subsequently resulting in acute coronary syndrome. *J Am Coll Cardiol*. 2009;54:49–57.
14. Min JK, Shaw LJ, Devereux RB, Okin PM, Weinsaft JW, Russo DJ, Lippolis NJ, Berman DS, Callister TQ. Prognostic value of multidetector coronary computed tomographic angiography for prediction of all-cause mortality. *J Am Coll Cardiol*. 2007;50:1161–1170.
15. Hoffmann H, Frieler K, Schlattmann P, Hamm B, Dewey M. Influence of statin treatment on coronary atherosclerosis visualised using multidetector computed tomography. *Eur Radiol*. 2010;20:2824–2833.
16. Itu L, Rapaka S, Passerini T, Georgescu B, Schwemmer C, Schoebinger M, Flohr T, Sharma P, Comaniciu D. A machine-learning approach for computation of fractional flow reserve from coronary computed tomography. *J Appl Physiol (1985)*. 2016;121:42–52.
17. Lee JM, Choi G, Koo BK, Hwang D, Park J, Zhang J, Kim KJ, Tong Y, Kim HJ, Grady L, et al. Identification of high-risk plaques destined to cause acute coronary syndrome using coronary computed tomographic angiography and computational fluid dynamics. *JACC Cardiovasc Imaging*. 2019;12:1032–1043.
18. Stone NJ, Robinson JG, Lichtenstein AH, Bairey Merz CN, Blum CB, Eckel RH, Goldberg AC, Gordon D, Levy D, Lloyd-Jones DM, et al. 2013 ACC/AHA guideline on the treatment of blood cholesterol to reduce atherosclerotic cardiovascular risk in adults: a report of the American College of Cardiology/American Heart Association Task Force on Practice Guidelines. *Circulation*. 2014;129:S1–S45.
19. Nissen SE, Nicholls SJ, Sipahi I, Libby P, Raichlen JS, Ballantyne CM, Davignon J, Erbel R, Fruchart JC, Tardif JC, et al. Effect of very

high-intensity statin therapy on regression of coronary atherosclerosis: the ASTEROID trial. *JAMA*. 2006;295:1556–1565.
20. Nicholls SJ, Ballantyne CM, Barter PJ, Chapman MJ, Erbel RM, Libby P, Raichlen JS, Uno K, Borgman M, Wolski K, et al. Effect of two intensive statin regimens on progression of coronary disease. *N Engl J Med*. 2011;365:2078–2087.
21. Ahmadi A, Stone GW, Leipsic J, Serruys PW, Shaw L, Hecht H, Wong G, Nørgaard BL, O'Gara PT, Chandrashekhar Y, et al. Association of coronary stenosis and plaque morphology with fractional flow reserve and outcomes. *JAMA Cardiol*. 2016;1:350–357.
22. Badeer HS. Hemodynamics for medical students. *Adv Physiol Educ*. 2001;25:44–52.
23. Inoue K, Motoyama S, Sarai M, Sato T, Harigaya H, Hara T, Sanda Y, Anno H, Kondo T, Wong ND, et al. Serial coronary CT angiography-verified changes in plaque characteristics as an end point: evaluation of effect of statin intervention. *JACC Cardiovasc Imaging*. 2010;3:691–698.
24. Raggi P, Davidson M, Callister TQ, Welty FK, Bachmann GA, Hecht H, Rumberger JA. Aggressive versus moderate lipid-lowering therapy in hypercholesterolemic postmenopausal women: Beyond Endorsed Lipid Lowering with EBT Scanning (BELLES). *Circulation*. 2005;112:563–571.
25. Callister TQ, Raggi P, Cooil B, Lippolis NJ, Russo DJ. Effect of HMG-CoA reductase inhibitors on coronary artery disease as assessed by electron-beam computed tomography. *N Engl J Med*. 1998;339: 1972–1978.

SUPPLEMENTAL MATERIAL

Data S1.

CT-based plaque analysis

The plaque characterization was performed according to CCTA findings and included various parameters which are mentioned as follows: 1) Minimal lumen diameter was manually measured with a digital caliper at the narrowest level of the lesion using the cross-sectional images; 2) Diameter stenosis was calculated as (reference diameter – minimal lumen diameter) / reference diameter and was measured manually with a digital caliper at the narrowest level of the lesion and the proximal reference on the cross-sectional images; 3) Lesion length was measured on curved planar reformation images at best projection view, from the proximal shoulder of plaque to the distal shoulder; 4) Remodeling index was defined as a maximal lesion vessel diameter divided by proximal reference vessel diameter, with positive remodeling (PR) defined as a remodeling index ≥ 1.1; 5) Low-attenuation plaque (LAP) was defined as any voxel < 30 HU within a coronary plaque, using a dedicated plaque analysis software (Coronary Plaque Analysis, version 2.0, Siemens Healthineers); 6) Spotty calcification was defined by an intra-lesion calcific plaque < 3 mm in length that comprised < 90 degrees of the lesion circumference; 7) Napkin-ring sign (NRS) was characterized by a plaque core with low attenuation areas on CT surrounded by a rim-like area of higher attenuation as previously reported; 8) Total plaque volume was automatically measured using the dedicated plaque analysis software as mentioned above. Plaque border was manually adjusted if needed.

CT-FFR analysis

As introduced recently, we used a machine-learning based algorithm for FFR simulation (cFFR, version 3.0, Siemens Healthineers). It's an alternative to physics-based approach and can be used on-site to calculate FFR_{CT} value. It's trained using a synthetically generated database of 12,000 different anatomies of coronary arteries with randomly placed stenosis among different branches and bifurcations. A computational fluid dynamics (CFD) by solving reduced-ordered Navier-Stokes equations is applied to calculate the pressure and flow distribution for each coronary tree. Quantitative features of anatomy and computed FFR_{CT} value were extracted for each location along the coronary tree. Then deep machine learning model is trained by using a deep neural network with four hidden layers to learn the relationship between the FFR value and quantitative anatomic features.

For the on-site processing, after CCTA data were successfully loaded, the centerline and luminal contours for whole coronary tree were automatically generated. The centerline and luminal contour are fundamental and critical information for computing FFR value. They were manually adjusted when needed. Users then manually identified all stenotic lesions to extract their geometrical features required for cFFR algorithm. Finally, those data were input into the pre-learned model and cFFR was computed automatically at all locations in the coronary arterial tree, and the resulting values were visualized by color-coded 3D coronary maps.

Table S1. Intra-observer reproducibility.

	ICC	95%CI	* p value
Intra-observer 1			
Focal Agatston score	0.99	0.99 to 1.00	<0.001
MLD	0.97	0.96 to 0.99	<0.001
Diameter stenosis	0.96	0.94 to 0.97	<0.001
Total lesion length	0.97	0.96 to 0.98	<0.001
TPV	0.95	0.93 to 0.96	<0.001
Calcified PV	0.96	0.95 to 0.97	<0.001
No-calcified PV	0.96	0.95 to 0.97	<0.001
LAP	0.98	0.97 to 0.99	<0.001
LAP volume	0.96	0.95 to 0.97	<0.001
Napkin-ring sign	0.97	0.96 to 0.98	<0.001
Spotty calcification	0.99	0.98 to 0.99	<0.001
Remodeling index	0.97	0.95 to 0.97	<0.001
△CT-FFR	0.98	0.98 to 0.99	<0.001
Intra-observer 2			
Focal Agatston score	0.99	0.98 to 1.00	<0.001
MLD	0.95	0.94 to 0.96	<0.001
Diameter stenosis	0.96	0.95 to 0.97	<0.001
Total lesion length	0.96	0.95 to 0.97	<0.001
TPV	0.97	0.96 to 0.98	<0.001
Calcified PV	0.97	0.96 to 0.98	<0.001
No-calcified PV	0.96	0.95 to 0.97	<0.001
LAP	0.98	0.96 to 1.00	<0.001
LAP volume	0.96	0.95 to 0.97	<0.001
Napkin-ring sign	0.97	0.96 to 0.98	<0.001
Spotty calcification	0.97	0.96 to 0.98	<0.001
Remodeling index	0.96	0.95 to 0.97	<0.001
△CT-FFR	0.98	0.96 to 1.00	<0.001

CI= Confidence interval; ICC= Intraclass correlation coefficient; LAP= Low attenuation plaque; MLD= minimal lumen diameter; PV= plaque volume; TPV= total plaque volume.

Table S2. Inter-observer reproducibility.

	ICC	95%CI	* p value
Focal Agatston score	0.99	0.98 to 1.00	<0.001
MLD	0.94	0.93 to 0.96	<0.001
Diameter stenosis	0.92	0.90 to 0.94	<0.001
Total lesion length	0.92	0.90 to 0.94	<0.001
TPV	0.94	0.90 to 0.96	<0.001
Calcified PV	0.94	0.92 to 0.95	<0.001
No-calcified PV	0.92	0.90 to 0.94	<0.001
LAP	0.97	0.95 to 0.98	<0.001
LAP volume	0.93	0.90 to 0.94	<0.001
Napkin-ring sign	0.96	0.94 to 0.97	<0.001
Spotty calcification	0.96	0.94 to 0.97	<0.001
Remodeling index	0.92	0.90 to 0.94	<0.001
△CT-FFR	0.96	0.95 to 0.97	<0.001

CI= Confidence interval; ICC= Intraclass correlation coefficient; LAP= Low attenuation plaque; MLD= minimal lumen diameter; PV= plaque volume; TPV= total plaque volume.

Figure S1. Bland-Altman analysis of measurement difference of △CT-FFR between observer 1 and observer 2.

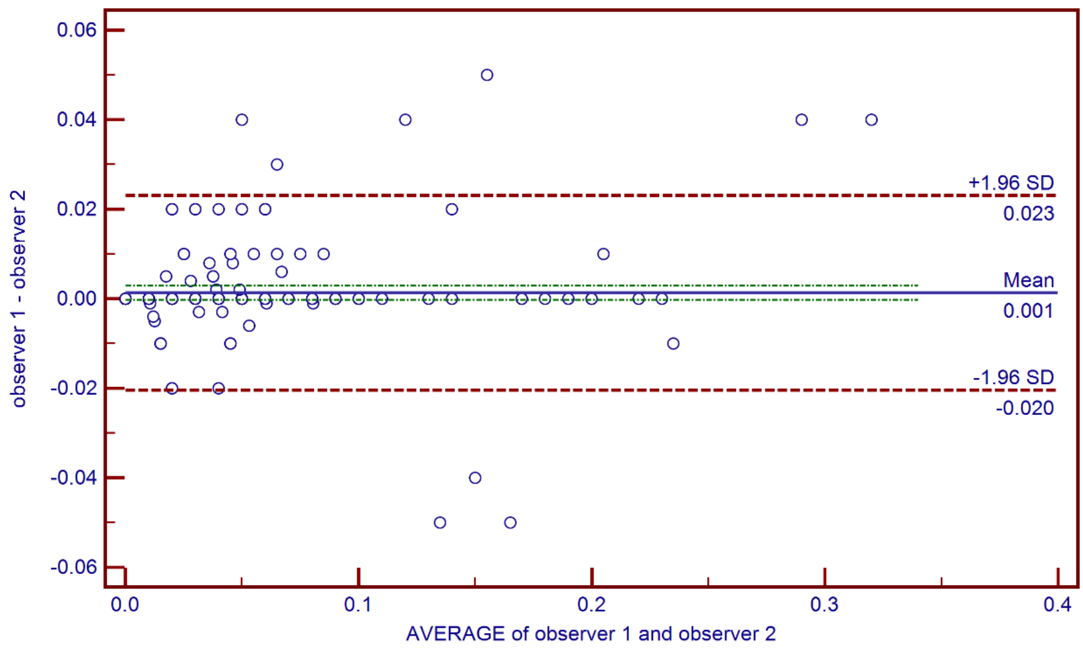

CT= computed tomography, FFR= fractional flow reserve